GA–A25671

DEPENDENCE OF CONFINEMENT AND STABILITY ON VARIATION OF THE EXTERNAL TORQUE IN THE DIII-D TOKAMAK

by
T.C. LUCE, K.H. BURRELL, R.J. BUTTERY, J.C. DeBOO, J.R. FERRON,
A.M. GAROFALO, P. GOHIL, D.A. HUMPHREYS, G.L. JACKSON,
R.J. JAYAKUMAR, J.E. KINSEY,[¶] R.J. LA HAYE, G.R. McKEE, M. OKABAYASHI,
C.C. PETTY, P.A. POLITZER, H. REIMERDES, D.J. SCHLOSSBERG, J.T. SCOVILLE,
M.W. SHAFER, W.M. SOLOMON, E.J. STRAIT, and F. VOLPE

NOVEMBER 2006

GENERAL ATOMICS

DISCLAIMER

GA–A25671

DEPENDENCE OF CONFINEMENT AND STABILITY ON VARIATION OF THE EXTERNAL TORQUE IN THE DIII-D TOKAMAK

by

T.C. LUCE, K.H. BURRELL, R.J. BUTTERY,* J.C. DeBOO, J.R. FERRON, A.M. GAROFALO,† P. GOHIL, D.A. HUMPHREYS, G.L. JACKSON, R.J. JAYAKUMAR,‡ J.E. KINSEY,¶ R.J. LA HAYE, G.R. McKEE,§ M. OKABAYASHI,# C.C. PETTY, P.A. POLITZER, H. REIMERDES,† D.J. SCHLOSSBERG,§ J.T. SCOVILLE, M.W. SHAFER,§ W.M. SOLOMON,# E.J. STRAIT, and F. VOLPE ∞

This is a preprint of a paper to be presented at the 21st IAEA Fusion Energy Conference, October 16-21, 2006, in Chengdu, China, and to be published in the *Proceedings.*

*Euratom/UKAEA Association, Culham, United Kingdom.
†Columbia University, New York, New York, USA
‡Lawrence Livermore National Laboratory, Livermore, California, USA.
¶Lehigh University, Bethlehem, Pennsylvania, USA.
§University of Wisconsin, Madison, Wisconsin, USA.
#Princeton Plasma Physics Laboratory, Princeton, New Jersey, USA.
∞Southwest Institute of Physics, Chengdu, China.

Work supported by
the U.S. Department of Energy
under DE-FC02-01ER54698, DE-FG02-89ER53297, W-7405-ENG-48, DE-FG02-92ER54141, DE-FG02-89ER53296, and DE-AC02-76CH03073

GENERAL ATOMICS PROJECT 30200
NOVEMBER 2006

Dependence of Confinement and Stability on Variation of the External Torque in the DIII-D Tokamak

T.C. Luce 1), K.H. Burrell 1), R.J. Buttery 2), J.C. DeBoo 1), J.R. Ferron 1), A.M. Garofalo 3), P. Gohil 1), D.A. Humphreys 1), G.L. Jackson 1), R.J. Jayakumar 4), J.E. Kinsey 5), R.J. La Haye 1), G.R. McKee 6), M. Okabayashi 7), C.C. Petty 1), P.A. Politzer 1), H. Reimerdes 3), D.J. Schlossberg 6), J.T. Scoville 1), M.W. Shafer 6), W.M. Solomon 7), E.J. Strait 1), and F. Volpe 8)

1) General Atomics, San Diego, California, USA
2) Euratom/UKAEA Association, Culham, United Kingdom
3) Columbia University, New York, New York, USA
4) Lawrence Livermore National Laboratory, Livermore, California, USA
5) Lehigh University, Bethlehem, Pennsylvania, USA
6) University of Wisconsin, Madison, Wisconsin, USA
7) Princeton Plasma Physics Laboratory, Princeton, New Jersey, USA
8) Max Planck Gesellschaft, München, Germany

e-mail contact of main author: luce@fusion.gat.com

Abstract. Modifications of the DIII-D tokamak and neutral beam injection (NBI) system now allow experiments on the energy confinement and global stability with variations in the external torque input. The external torque can vary in the range -4 to 4 Nm at a constant NBI power of 5 MW, where positive torque corresponds to NBI in the same direction as the plasma current. Energy confinement in plasmas with an H-mode edge shows a significant increase (>50%) as the torque increases from balanced injection. H-mode discharges with negative torque and L-mode discharges with positive torque do not show similar increases in energy confinement over balanced injection. The new NBI configuration and new real-time spectroscopic analysis of the toroidal rotation allow simultaneous feedback control of the plasma stored energy and toroidal rotation. Strong variation of the L-H threshold power (a factor of 3) is observed as the NBI mixture is changed from counter-injection to co-injection. The onset pressure level and saturated amplitude of tearing modes are both observed to vary significantly (~50%) with the external torque. The rotational stabilization of resistive wall modes persists to much lower rotation frequencies using nearly balanced NBI than the critical frequency previously determined in experiments where the plasma rotation was slowed by resonant magnetic braking. Since the majority of the confinement and stability databases that comprise the ITER physics basis employ NBI with co-injection, the present results imply an examination of the implications of low rotation in ITER is warranted.

1. Introduction

Rotation and rotational shear of tokamak plasmas are both observed and expected from theoretical consideration to play a significant role in confinement and stability. A majority of the existing database on tokamak confinement and stability is derived from experiments with neutral beam injection (NBI) in the direction of the plasma current (co-injection) as the dominant source of heating. These discharges with co-injection typically have rotation frequencies in the kHz range. The first-generation burning plasma experiment ITER has a goal of an energy gain Q>10 [1], implying that the self-heating from charged fusion products will be twice the auxiliary heating. In addition to the lack of torque input from the self-heating, a majority of the initial complement of auxiliary heating power is planned to be wave heating with little torque input, and the NBI is being designed for much higher energy than present-day NBI with correspondingly lower torque for the same power. Given this and the much larger moment of inertia of the ITER plasma than present-day tokamaks, a significantly lower plasma rotation and rotational shear are expected in ITER.

Modification of the DIII-D NBI system and vacuum vessel during the 2005-2006 vacuum opening [2] has allowed a series of experiments to begin to assess the impact of rotation on several areas important to the prediction of ITER performance. The DIII-D NBI system consists of four beamlines capable of injecting power from two sources each. The sources are located horizontally on either side of the centerline of the beamlines, yielding one beam slightly more tangential than the other. At present, there are power supplies available to operate seven NBI sources with a nominal power of 2.5 MW each. The previous configuration had all beamlines oriented for co-injection. The recent modification re-oriented a single beamline with two sources for counter-injection. Therefore, comparative experiments with 5 MW can be carried out with co-, balanced or counter-injection, while experiments with balanced or co-injection at 10 MW can be compared. As a guideline, the tangential source at 80 kV gives about 1 N·m per 1 MW power. The more normal source gives about 65% of the torque of the tangential source. For the type of NBI sources used, the torque input varies with voltage as V^2, while the power varies as $V^{5/2}$. The allowed voltage range is 35-93 keV, so some variation of the torque/power ratio is possible from discharge to discharge. Co-injection will be considered positive torque by convention in this report.

The initial experiments reported here show clear trends in energy confinement, plasma stability, and the L-H power threshold as the input torque is varied. However, they have not been placed in the context of previous experiments, nor have the implications for ITER been fully explored. These areas have been left to more complete publications of the individual experiments. Also, the torque considered in this report is the simple linear momentum exiting the beamlines times the tangency radius of the launched beams, including some correction for half- and third-energy components of the beam. The more difficult question of evaluating the torque actually applied to the plasma or whether torque is the appropriate physical variable to consider is deferred to future publications.

In this report, Sec. 2 contains the experimental results on energy confinement and a brief discussion of momentum transport. Section 3 shows the new ability to impose simultaneous feedback control of the stored energy and toroidal rotation. Section 4 discusses how the L-H power threshold is changed by the mix of NBI. Section 5 gives results of changing torque on plasma stability. Finally, a summary is given in Sec. 6.

2. Energy Confinement

Experiments to measure the effect on energy confinement of varying the external torque input have been carried out in L-mode, H-mode, and advanced inductive (or hybrid) discharges. Figure 1 summarizes the dataset by plotting the thermal energy confinement time (τ_{th}) against the external torque input. In all cases, the input NBI power has not been corrected for shine through or first-orbit losses. However, the maximum correction is expected to be less than 10%, even for counter-injection, based on design calculations and on preliminary evaluation of discharges shown here using a full orbit-following Monte Carlo treatment of the ions generated by NBI. A correction of this magnitude would not alter the observations discussed here. The calculation of the thermal stored energy is based on a 0-D formula validated previously on DIII-D data.

The symbols connected by lines in Fig. 1 are scans where the toroidal field (B), plasma current (I), density (n), and stored energy (W) are held fixed as the external torque is varied. From the dimensionless parameter scaling perspective, these scans hold the normalized gyroradius (ρ^*), normalized pressure (β), safety factor (q), and collisionality (ν^*) fixed in global parameters, while the Mach number is varied. A local transport analysis to see if the profiles of the dimensionless parameters are fixed has not been completed. The variation among the scans shown within a single class of discharges are due to changes in B, I, n or W.

A significant increase in τ_{th} is seen going from balanced to co-injection for all three types of discharges with H-mode edge (standard, advanced inductive, and hybrid). In most cases, the increase in τ_{th} is >50%. As mentioned above, this variation with torque is much larger than that expected from neglect of prompt losses. The same variation in torque in L-mode results in no discernable change in the thermal confinement. Going from balanced to counter-injection in conventional H-mode results in only a slight decrease in τ_{th}.

One possible explanation for the improvement in confinement with larger torque input is the increase in the equilibrium ExB shear limiting the size of the turbulent eddies. This hypothesis was tested for one of the hybrid scenario scans. Figure 2 shows the time history of a typical discharge. The beginning has the standard hybrid startup with only co-injection [3]. At 3500 ms, both counter-injection sources are started while the co-injection sources remain under feedback control to maintain constant W (or β). The counter-injected power is modulated at fixed duty cycle, giving 3.2 MW with corresponding -1.1 Nm of torque. The co-injected power under feedback control gives about 4.8 MW of power and 3.0 Nm torque. The toroidal rotation responds to the changing torque input by slowing by about a factor of 10. The energy confinement is reduced, as indicated by the increased power required to maintain the same stored energy. To look for the significance of

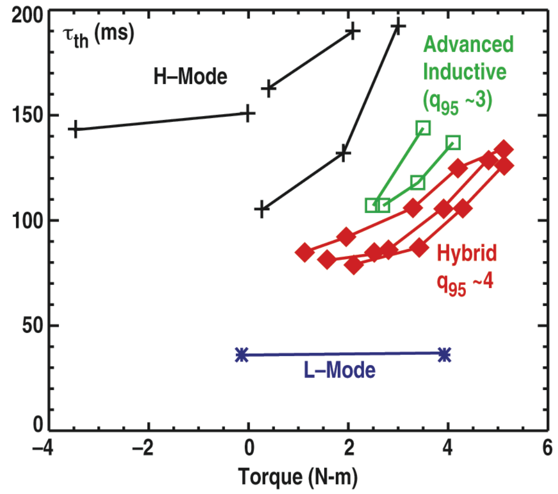

FIG. 1. Thermal energy confinement τ_{th} (ms) vs external torque input (N·m) for L mode (∗), standard H mode (+), advanced inductive (square), and hybrid candidate scenario (◊) discharges.

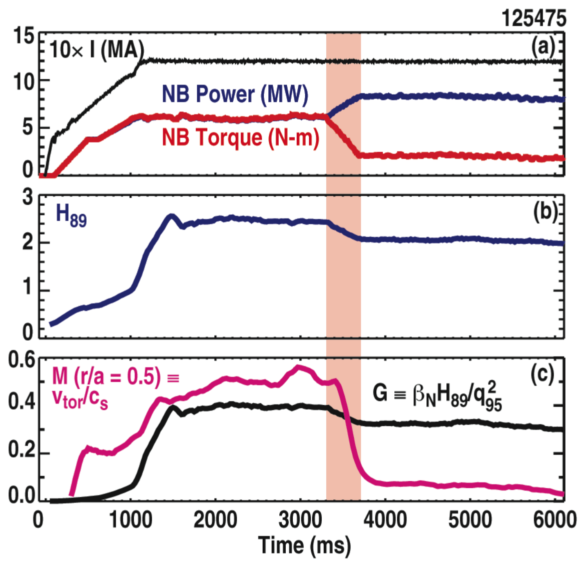

FIG. 2. Time histories for a q_{95} = 4.0 hybrid candidate scenario at β_N = 2.6 where the NBI mix was switched from all co-injection to more balanced injection at t = 3500 ms. (a) Plasma current x 10 (MA) (black), NBI power (MW) (blue), NBI torque (N·m) (red). The NBI power and torque are smoothed with a 200 ms moving average to see more clearly the trends. (b) Ratio of global energy confinement time to the ITER-89P confinement scaling. (c) Mach number (velocity normalized to ion sound speed) at the half-radius (magenta) and normalized fusion gain parameter ($G \equiv \beta_N H_{89}/q_{95}^2$) (black). The Mach number and G are smoothed with a 200 ms moving average to see more clearly the trends.

the equilibrium ExB shear in determining the transport, calculations of the electron and ion temperature profiles using the GLF23 transport model [4] with and without ExB shear were performed for times before and after the decrease in torque. Figure 3 shows that ExB shear has a significant effect in the co-injection case in the context of this model, while it plays only a minor role with more balanced injection. Starting with the measured density, current, and toroidal rotation profiles, this model does a good job of describing the change in transport when the effects of equilibrium ExB shear are included.

Momentum transport becomes an important issue for extrapolation of energy confinement to ITER if equilibrium ExB shear plays a significant role. Using the angular frequency at the half-radius as a proxy for a more detailed analysis, Fig. 4 shows some features that indicate a characterization of momentum transport will prove more difficult than that of energy transport. The dataset displayed is the same set of discharges shown in Fig. 1. The first observation is that discharges with very different thermal confinement have similar responses to external torque. (A proper analysis must include the mass of the rotating shell, but this difference is not enough to account for the observation.) Also, both L-mode and H-mode discharges have finite angular rotation frequency in the absence of external torque input [5,6]. This means that the concept of a momentum confinement time corresponding to global energy confinement time will not be valid in general. Finally, the hybrid discharges may exhibit a nonlinear response of the angular momentum to external torque. These discharges have m=3/n=2 tearing modes that may lead to two different effects with no analogue in energy transport. First, in a tokamak with non-circular cross section, the m=3/n=2 mode will have m=2/n=2 and m=4/n=2 sidebands that co-rotate with the q=3/2 surface. Due to plasma viscosity, these sidebands will transfer momentum between these surfaces. Second, the tearing modes can induce currents in the wall, leading to a transfer of momentum directly out of the plasma.

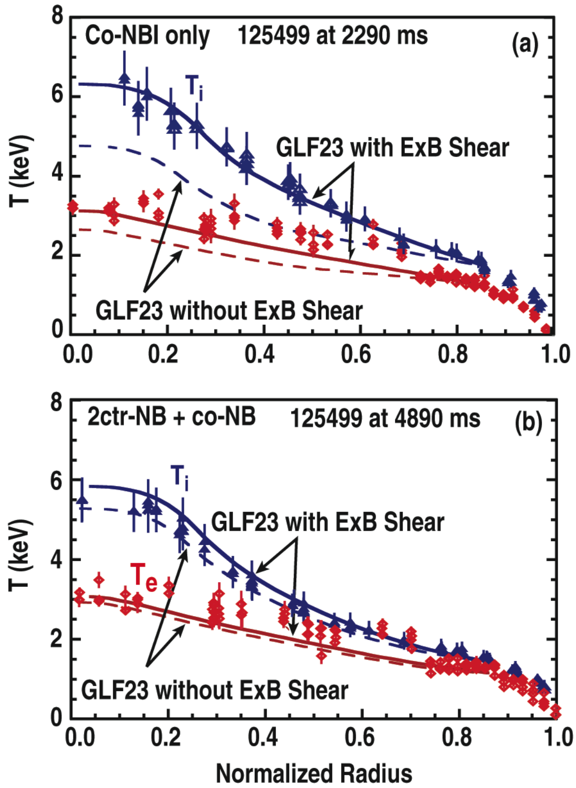

FIG. 3. Comparison of experimental ion (Δ) and electron (◊) temperature profiles with predictions using the GLF23 model with (solid) and without (dashed) ExB shear. Panel (a) shows the calculation for a time with pure co-injection., and panel (b) shows the calculation for a time with more balanced injection.

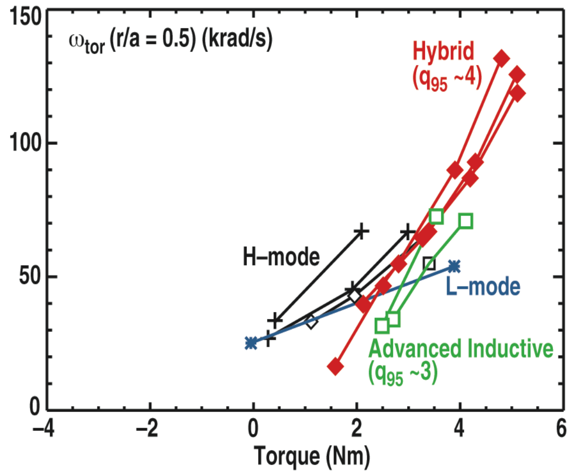

FIG. 4. Angular rotation frequency ω_{tor} (krad/s) vs external torque input (N·m) for L mode (∗), standard H mode (+), advanced inductive (square), and hybrid candidate scenario (◊) discharges.

Another source for nonlinearity is the effect of unintentional non-axisymmetric magnetic fields ("error fields") due to imperfections in assembly of the tokamak. As the plasma rotates faster, the skin effect reduces the influence of these error fields, leading to less drag. The presence of intrinsic rotation and these electromagnetic mechanisms for transferring momentum across or out of the plasma means that the tools used to characterize energy transport, such as global confinement time and local diffusivity, are not likely to lead to a sensible model for momentum transport.

3. Feedback Control

While energy and momentum transport are not yet predictable, the stored energy and toroidal rotation do exhibit a monotonic relation to power and torque, respectively, within reasonable operational limits. This implies that feedback control can be established, if real-time sensors exist. Feedback control of stored energy has been routine for many years in the DIII-D tokamak, but the new ability to analyze spectroscopic data in real-time, coupled with the new NBI configuration, now allows simultaneous feedback control of stored energy and rotation. Figure 5 shows two examples of this. In the example on the left, the stored energy is held constant after 2700 ms, while the rotation request has a step increase at 4000 ms. As expected the torque required increases. The power required to maintain fixed stored energy decreases, consistent with the discussion of the previous section. In the example on the right, the stored energy request is increased at 3400 ms, while the rotation request is constant. As expected, the power required increases but surprisingly, the torque to maintain the toroidal rotation is fixed. Since density is held constant, the stored energy increase corresponds to a temperature increase. The independence of momentum transport from temperature is further indication that treating momentum transport by analogy to energy transport will probably not be fruitful.

The controllers for both quantities are Proportional-Integral controllers. The gains were determined by modeling prior to the experiment and not optimized further [7]. While it is likely that these gains can be further optimized empirically, the ability to predict the gains

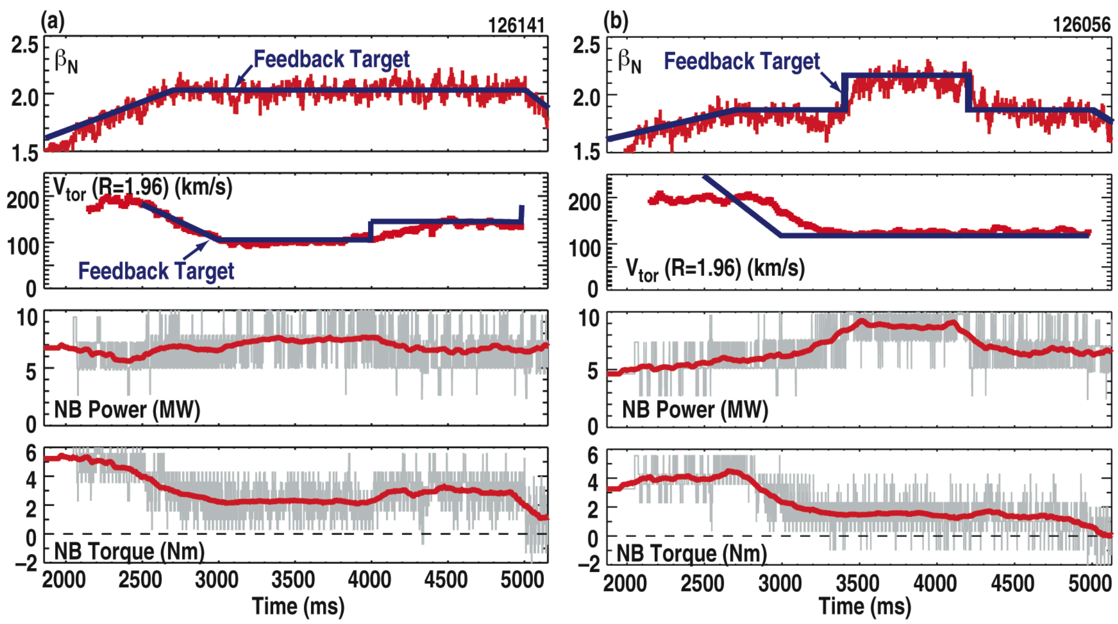

FIG. 5. Demonstration of independent feedback control of stored energy and toroidal rotation. (a) Stored energy constant, toroidal rotation changed. (b) Stored energy changed, toroidal rotation constant. The gray traces in the NB power and torque graphs are the actual signals, while the red traces are smoothed with a 200 ms moving average to show more clearly the trends.

from open-loop experiments significantly reduces the experimentation time needed to implement new controllers.

4. L-H Power Threshold

All proposed burning plasma scenarios, including those for ITER, anticipate an H-mode edge transport barrier. This means that accurate prediction of the power required to reach H-mode operation is key to validating scenarios. Experiments have been carried out in the DIII-D tokamak examining the variation of the power to achieve an L-H transition as a function of the NBI external torque, although torque has not been identified as the correct physical parameter responsible for the observed variations. The experiments were performed in a single day to minimize the effects of variations in wall conditions. The power threshold was determined by making small changes in power by either changing the modulation frequency or by changing the acceleration energy of the NBI. The modulation time scale is less than the fast-ion slowing-down time, and the time-averaged power is held fixed for many confinement times before the increase to the next power level.

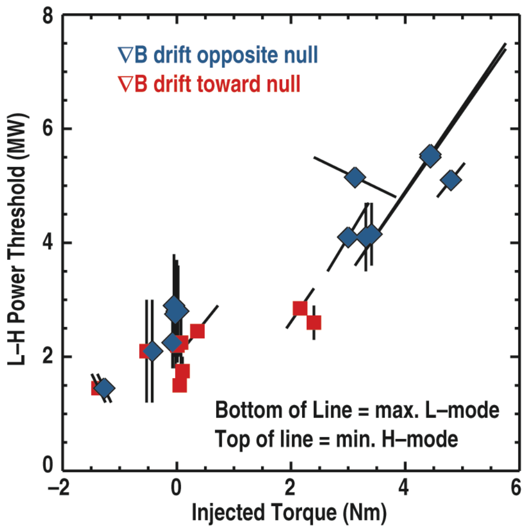

FIG. 6. L-H power threshold (MW) vs external torque input (N·m) for ion ∇B drift toward (square) and away (diamond) from the active null. The bottom of the lines on the plot indicate the highest power case in the power ramp that remained in L mode. The top of the lines on the plot indicate the power and torque of the next step which caused H mode. A vertical line indicates the power was increased with no change in torque; a slanted line indicates both power and torque changed.

The experiments show a striking trend in the L-H power threshold with changes in the external torque, as seen in Fig. 6. Across the range in external torque, the threshold power varies by more than a factor of 3. At low external torque input, there is little difference in the L-H threshold power as the plasma shape is changed from having the ion ∇B drift toward or away from the active null. (The plasma geometry has a null at both ends vertically, but the plasma is biased either up or down by >3 cm, making one of the nulls active.) Typically with only co-injection, a difference in threshold power of about a factor of 2 has been observed with the threshold lower in the case where the ion ∇B drift is in the direction of the active null [8].

A theoretical explanation of this strong dependence of the L-H power threshold on the NBI geometry is not available at present. One obvious hypothesis is the variation of the prompt orbit losses with NBI geometry. Previous experiments on DIII-D discounted this hypothesis; however, the present data set should provide a strong test of this and any other hypotheses. The experiment was designed to obtain detailed fluctuation and radial electric field information at the edge, and these data are presently under analysis.

5. Stability

The recent DIII-D experiments indicate a strong influence of rotation on both tearing mode and resistive wall mode (RWM) stability. Tearing modes are expected to be the pressure-limiting instability in both the conventional H-mode and hybrid operation in ITER. The RWM is expected to be the principal limitation on the pressure in the steady-state scenarios.

5.1. Tearing Modes

The onset of the m=2/n=1 tearing mode represents the limit to increasing the pressure in conventional H-mode scenarios. Modes with higher n occur at lower pressure and cause a reduction in confinement, but the m=2/n=1 tearing mode can lead to a major disruption, especially when it locks. Experiments with slow increments in power (similar to the L-H threshold experiments described in the previous section) have been used to determine the pressure at which the m=2/n=1 mode appears as a function of the plasma rotation. The normalized β ($\beta_N \equiv \beta/(I/aB)$ in % mT/MA) is used to quantify the pressure even though I, a, and B are held fixed. There is about a 50% increase in the β_N at which the mode appears as the plasma rotation varies from -5 kHz to 5 kHz (Fig. 7), where the positive frequency is co-rotation as in the sign convention for the torque. The local frequency at *q*=2 is determined by the laboratory frame frequency of the mode at onset. Above 5 kHz, there appears to be little increase in the β_N at which the mode appears. To eliminate the possible effects of uncompensated n=1 error fields, the pressure limit was determined in the presence of large intentional error fields. The change in the β_N at onset was much smaller than the variation seen in Fig. 7 with optimal compensation. This and the asymmetric response around a zero frequency, indicate static error fields are not playing a significant role in the observed trend. The influence of the change in current driven by NBI on the total current profile is believed to be small, due to the small fraction of the total current calculated to be due to NBI, but the effect of this on the classical tearing stability index (Δ´) is not yet quantified.

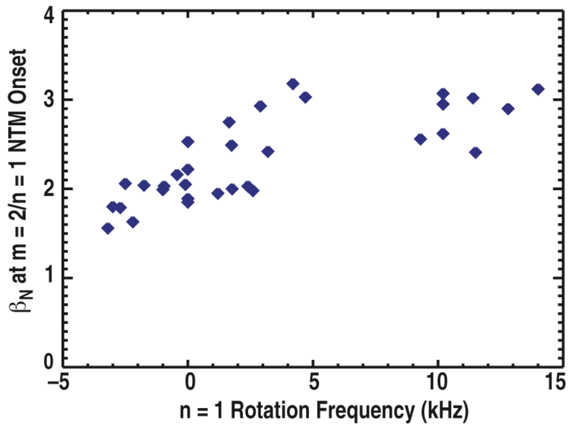

FIG. 7. Pressure at which an m=2/n=1 tearing mode occurred vs the rotation frequency of the mode at onset (kHz). The pressure is quantified as normalized β [$\beta_N \equiv \beta/(I/aB)$]. Discharges are conventional H mode at q_{95} = 4.5 with sawteeth.

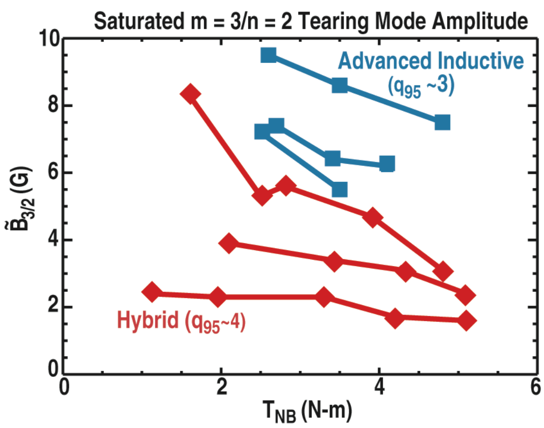

FIG. 8. Variation of the saturated m=3/n=2 tearing mode amplitude measured at the wall (G) vs the external NB torque input (N-m). Both advanced inductive (q_{95}~3) (blue square) and hybrid candidate (q_{95}~4) (red diamond) scenario discharges are shown.

Hybrid scenario discharges have a saturated m=3/n=2 tearing mode that seems to play a key role in bringing the current profile to a stationary condition that is favorable to both m=2/n=1 stability and energy confinement [9]. As shown in Fig. 8, the saturated amplitude of this mode shows a dependence on the external torque. This may be explained by the skin effect limiting the mode amplitude by limiting the growth of m=2/n=2 and m=4/n=2 sidebands co-rotating with the m=3/n=2 mode. This hypothesis requires differential rotation at the various rational surfaces. As in the case of the m=2/n=1 mode, the influence of the changing current drive due to NBI on Δ´ has not been quantified, but is again expected to be small.

5.2. *Resistive Wall Modes*

The RWM is a mode that appears below the ideal wall kink limit due to the finite resistivity of the wall. With sufficient rotation (and torque input), the wall appears ideal to the plasma, and the pressure limit is again the ideal limit. In the absence of sufficient rotation, the wall still slows the growth enough to allow direct feed-back control of the RWM with an appropriate coil and power supply set. A key research area is to determine how much rotation is sufficient. Previous experiments in DIII-D used resonant magnetic braking with an n=1 dominant spectrum to slow the plasma to determine the rotational threshold [10,11]. The recent modifications to the DIII-D NBI system allow similar low rotation experiments, but with optimal correction of n=1 error fields. The results shown in Fig. 9 indicate that the recent low torque input cases are stable to the ideal kinetic mode at much smaller rotation frequency [12]. The use of an n=1 resonant perturbation to slow the plasma evidently leads to interaction with plasma that is not exclusively due to the RWM. Preliminary modeling of the recent low torque experiments indicates the kink damping model in the MARS-F calculation agrees with the recent data [13]. A low rotational stabilization threshold is encouraging for burning plasma experiments with steady-state scenarios and much lower torque input than present-day experiments.

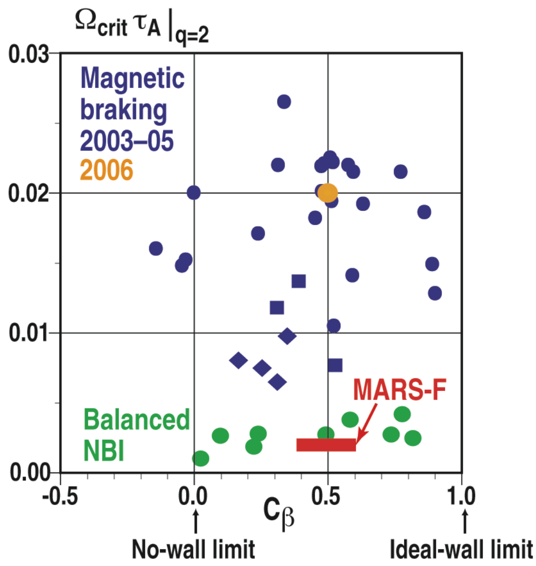

FIG. 9. Threshold for rotational stabilization of the RWM vs the normalized pressure β_N relative to the no-wall and ideal wall β limits. Data obtained from resonant n=1 magnetic braking are shown in blue and orange; data obtained with low torque input are shown in green. The MARS-F calculation shown in red indicates the marginal stability point obtained by scaling the experimental rotation profile.

6. Summary and Discussion

Significant variations in energy confinement in plasmas with H-mode edge, in L-H power threshold, and in plasma stability are observed in DIII-D when using the new NBI configuration to vary the external torque input. Increasing the torque from balanced injection to co-injection leads to an increase in thermal energy confinement of >50% in many cases. The L-H power threshold shows more than a factor of 3 increase going from pure counter-injection to pure co-injection. The onset pressure for a m=2/n=1 tearing mode rises from β_N=2 to β_N=3 in a similar scan from counter-injection to co-injection. These experiments indicate that relying solely on co-injection data to project to ITER or other burning plasma scenarios may result in a systematic bias, if similar rotation cannot be obtained in these future plasma experiments. This makes prediction of momentum transport a key issue; however, preliminary observations discussed here indicate that the tools developed for analysis of energy confinement are not likely to be applicable to the study of momentum transport.

Acknowledgment

This work was supported by the U.S. Department of Energy under DE-FC02-04ER54698, DE-FG02-89ER53297, W-7405-ENG-48, DE-FG02-92ER54141, DE-FG02-89ER53296, and DE-AC02-76CH03073.

References

[1] AYMAR, R., et al., Plasma Phys. Control. Fusion **44** (2002) 519.
[2] SCOVILLE, J.T., et al., "Rotation of a Neutral Beamline to Obtain Counter-Injection on the DIII-D Tokamak," submitted to Fusion Sci. Technol (2006).
[3] LUCE, T.C., et al., Phys. Plasmas **11** 92004) 2627.
[4] KINSEY, J.E., et al., Phys. Plasmas **12** (2005) 052503.
[5] RICE, J.E., et al., Nucl. Fusion **45** (2005) 251.
[6] deGrassie, J.S., et al., Phys. Plasmas **11** (2004) 4323.
[7] SCOVILLE, J.T., et al., "Simultaneous Feedback Control of Plasma Rotation and Stored Energy on the DIII-D Tokamak," submitted to Fusion Eng. Design (2006).
[8] CARLSTROM, T.N., et al., Plasma Phys. Control. Fusion **44** (2002) A333.
[9] WADE, M.R., et al., Nucl. Fusion **45** (2005) 407.
[10] LA HAYE, R.J., et al., Nucl. Fusion **44** (2004) 1197.
[11] REIMERDES, H., et al., Nucl. Fusion **45** (2005) 368.
[12] GAROFALO, A.M., et al., this conference.
[13] REIMERDES, H., et al., "Reduced Critical Rotation for Resistive Wall Mode Stabilization in a Near-Axisymmetric Configuration," submitted to Phys. Rev. Lett. (2006).